Int. J. Electrochem. Sci., 14 **(2019)** 8405 – 8418, doi: 10.20964/2019.09.41

International Journal of
ELECTROCHEMICAL
SCIENCE
www.electrochemsci.org

Rose, Gardenia, and Solanum Violaceum Extracts as Inhibitors of Steel Corrosion

Xia Wang[1*], *Yue Gu*[1*], *Qiao Zhang*[1], *Linglong Xu*[1], *Xiong Li*[1]

School of Material Science and Engineering, Southwest Petroleum University, Chengdu, Sichuan
[*]E-mail: swpi_wx@126.com, 2871765615@qq.com

Received: 30 April 2019 / *Accepted:* 3 July 2019 / *Published:* 31 July 2019

To explore the application of environmentally friendly metal corrosion inhibitors, we made extracts of three kinds of plant corrosion inhibitors, and we explored ways to improve their corrosion inhibition efficiency. We used the weight loss method to study the corrosion inhibition of mild steel in 1 M HCl solutions, using extracts of rose, gardenia, and Solanum violaceum. We found that the extracts acted as effective corrosion inhibitors for mild steel in an acidic medium. The inhibition process was attributed to the formation of an adsorbed film of inhibitor on the metal surface that protected the metal against corrosion. We determined by Fourier infrared spectroscopy that the N-H, C=N, and C-O functional groups in the three plant extracts were important is this corrosion inhibition. The inhibition efficiency (%E) of the extracts increased with increasing inhibitor concentration but decreased with increasing temperature. Using electrochemical methods, we found that the three plant corrosion inhibitors researched are all mixed corrosion inhibitors, which have inhibitory effects on both the cathodic and anodic reaction processes. Mixtures of (1) gardenia blossom inhibitor (GD) with rose extract inhibitor (RE) and (2) Solanum violaceum inhibitor (SV) with RE had synergistic effect factors less than one, which implied that the synergistic effect was great, and that the efficiency of a single plant inhibitor RE was improved by mixing with other inhibitors.

Keywords: Plant corrosion inhibitor; gardenia; rose; Solanum violaceum

1. INTRODUCTION

In industrial production and modern life, corrosion damage is a significant issue that we cannot ignore. The use of corrosion inhibitors in metal pickling is one response to this problem due to the simplicity of the process and its low cost [1]. Traditional corrosion inhibitors are generally toxic organic compounds [2], but there are non-toxic and otherwise harmless green corrosion inhibitors that include natural polymer derivatives [3-5] and natural plant extracts [6-8]. Natural plant corrosion inhibitors are especially attractive because they are widely available and are environmentally friendly, however they have low corrosion inhibition efficiency, poor stability, and poor after-effects [9-11].

In order to improve the performance of plant corrosion inhibitors [12,13], we used combinations of plant extracts. Rose [14,15], gardenia [16,17] and Solanum violaceum [18,19] are three plants that are readily available in large quantities. They contain amino acids, fatty acids, flavonoids, steroids, and other organic substances, and they are widely used in ornamental greening and medicine. We prepared extracts of Solanum violaceum, gardenia, and rose to be used as plant corrosion inhibitors by the Soxhlet extraction method [20]. We tested the corrosion inhibition performance of the extracts on A3 steel in 1 M HCl solution to determine whether combinations of these extracts would improve the performance compared to single extracts. Our goal was to develop efficient, economical, and non-polluting rose, gardenia and Solanum violaceum corrosion inhibitors for the pickling industry.

2. MATERIALS AND METHODS

2.1. Preparation of the Plant Corrosion Inhibitors

Fresh roses, gardenias, and Solanum violaceum were collected, impurities were removed, and they were cleaned, dried in the shade, dried in an oven at 40 ^{o}C, ground into powder, sifted, and stored in sealed bags.

Plant powder samples with a mass of 2.0 g were extracted for 8 h in a Soxhlet extractor with 250 mL of deionized water in a constant temperature oil bath at 100 ^{o}C. We used the final solution as the corrosion inhibitor. The difference in the mass of the dry filter paper bag before and after extraction was used to calculate the concentration (C) of the solution. In this way, rose extract inhibitor (RE), gardenia blossom inhibitor (GD), and Solanum Violaceum inhibitor (SV) were prepared.

C is defined as:

$$C = \frac{(w_f + w_p) - w_b}{v_L} \quad (1)$$

w_f (w_p)is the quality of filter paper (plant powder), w_b is the quality of filter paper package after plant extraction and drying, v_L is the volume of liquid obtained by extraction. Table 1 data shows A3 steel composition.

Table 1. A3 steel composition

Comment	C	Si	Mn	P	S	Al	Ni	Cr	Cu
wt%	0.22	0.30	1.40	0.045	0.005	-	0.01	0.01	-

2.2. Performance evaluation methods

We used infrared spectroscopy (Nicolet 6700) to analyze sample compositions. The experimental extraction products (RE, GD, and SV) were added to the surface of KBr plates and placed in the IR spectrometer to determine the functional groups present and help us to analyze the importance of the groups in the extracts corrosion inhibition performance.

Corrosion rate (V_{corr}) and inhibition efficiency (η) were measured by weight loss test. Our mild steel samples for weight loss test were standard A3 steel with dimensions of 30 mm×15 mm×2 mm. At least three parallel experiments were carried out under the same experimental conditions, and measurements without obvious errors were averaged. The corrosion medium was 200 mL of a 1 mol/L HCl solution. After 4 hours in a constant temperature water bath, the test samples were removed, dried, and weighed.

V_{corr} and η were defined as:

$$V_{corr} = \frac{W_0 - W_1}{St} \quad (2)$$

W_0 (W_1) is the quality of A3 steel before (after) corrosion. S is the surface area exposed to solution. T is the soaking time.

$$\eta = \frac{V_{corr}^0 - V_{corr}^{inh}}{V_{corr}^0} \times 100\% \quad (3)$$

V_{corr}^0 (V_{corr}^{inh}) is the uninhibited (inhibited) corrosion rate.

The parameters for our AC impedance test were 5 mV, scanning frequency signals of 0.01 Hz to 100 kHz, and polarization curve parameters of scanning rate of 0.5 mV/s and scanning interval of -0.3 V to 0.3 V (relative to the open circuit potential). The experimental temperatures were all 30 ºC. In order to ensure the accuracy of the data, the experiment for each group was repeated more than three times. The size of the A3 steel samples for electrochemical testing were 10 mm×10 mm×3 mm, with AB adhesive polytetrafluoroethylene (PTFE) on all surfaces except a 1 cm^2 section.

After polishing, the A3 steel sheets were put into a 1 mol/L HCl solution at 30 ºC with different concentrations (0.2g/L, 0.6g/L and 1g/L) respectively, soaking 4 hours and then scanning by EVO-MA15 electron microscopy observation.

3. RESULTS AND DISCUSSION

Fig. 1 shows the infrared spectra for RE, GD, and SV. Fig 1(a) shows the stretching vibration of O-H and N-H near the wave number 3405.67 cm^{-1}, the skeleton vibration of C=N and aromatic rings at 1722.12 cm^{-1}, and the absorption peaks of C-O at 1623.769 cm^{-1}, 222.648 cm^{-1}, and 1051.014 cm^{-1}. Fig 1(b) shows the stretching vibration peaks of O-H (association) and N-H at wave number of 3415.31 cm^{-1} and the stretching vibration absorption peaks of C=O, C=C, or C=N at wave number of 3415.31 cm^{-1}. The vibration absorption peak of carboxylate C=O and the stretching vibration peak of C=C or C=N appeared at 1625.69 cm^{-1}, and the vibration peak of C-C or C-O was at 1103.08cm^{-1}. Fig. 1(c) shows the stretching vibrations of O-H and N-H that occur at 3426.10 cm^{-1}, the stretching vibrations of accumulative double bonds of N=C=S that occur near 2103.97 cm^{-1}, and the stretching vibrations of C=S and S=O near 1045.63 cm^{-1}.

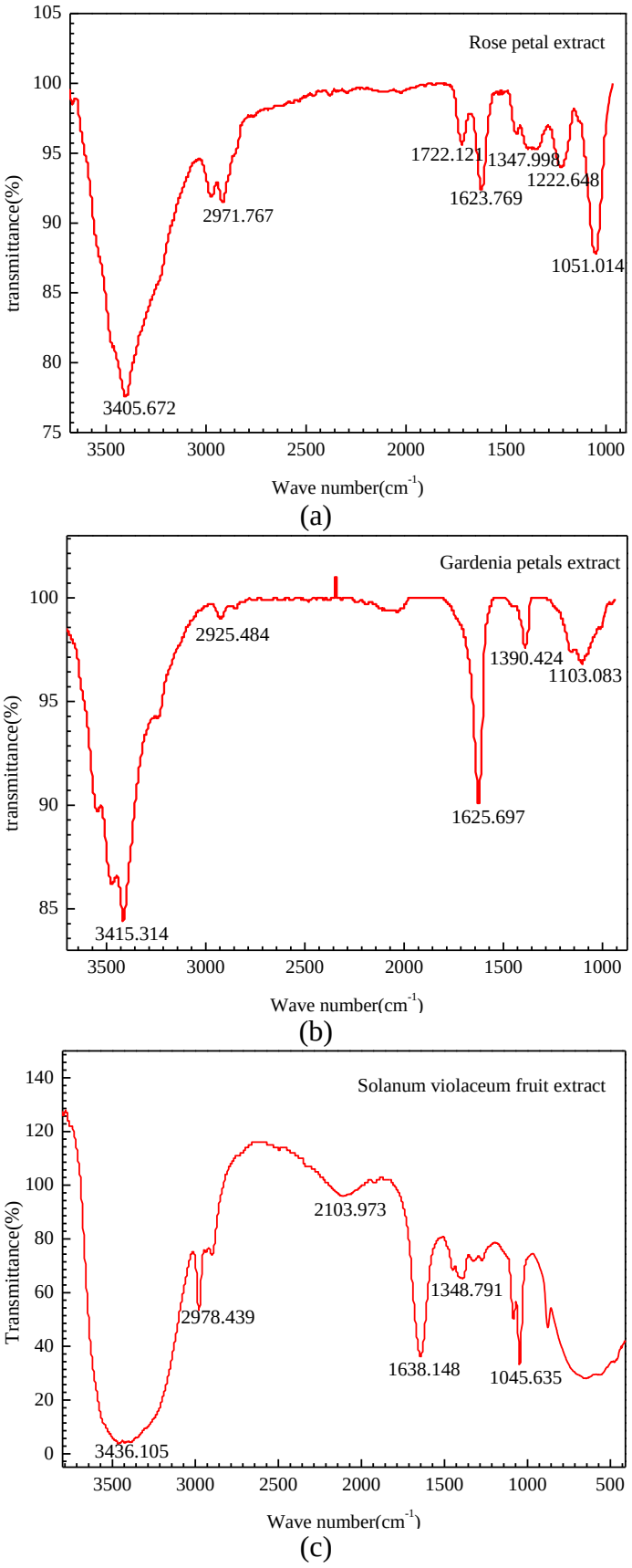

Figure 1. Infrared spectra for RE(a), GD(b), and SV(c).

Substances containing polar groups are easy to protonate in acid solution [21]. Substances in RE, GD, and SV can be adsorbed by the metal surface in several ways. The lone pair electrons of O, N, and S atoms can form coordinate covalent bonds to the metal surface. The substances can also be adsorbed on the metal surface due to electrostatic action or the formation of chelates with Fe^{3+}. In addition, extracts containing double bonds can be attracted to the metal surface. In this way, the adsorbed substances in RE, GD, and SV can inhibit the corrosion of A3 steel.

Figure.2 shows that the inhibition efficiency of RE, GD, and SV all initially increased with increasing temperature, followed by a decrease with increasing temperature above a certain temperature. The inhibition efficiency of GD and SV on A3 steel in 1 mol/L HCl solution reached the highest at 50 ºC (86.22% for GD and 89.30% for SV). When the temperature was more than 50 ℃, the GD and SV corrosion inhibition effects had a declining trend. For RE, the highest inhibition effect of 75.57% was at 40 ºC. At temperatures higher than 40 ºC, the inhibition effect of RE on A3 steel decreased. One reason is that increasing temperature accelerates the motion of molecules, and at some temperature, the increased motion makes the desorption rate of the corrosion inhibitors on the steel surface higher than the adsorption rate, which exposes part of the surface of A3 steel to the corrosive environment. High temperature will also destroy the effective components in RE, GD and SV, resulting in a less effective corrosion inhibition. From Fig.2, we can see that GD and SV have better high temperature resistance than RE at the same concentration. The corrosion rate and inhibition efficiency were calculated by Eqs.2 and 3, respectively.

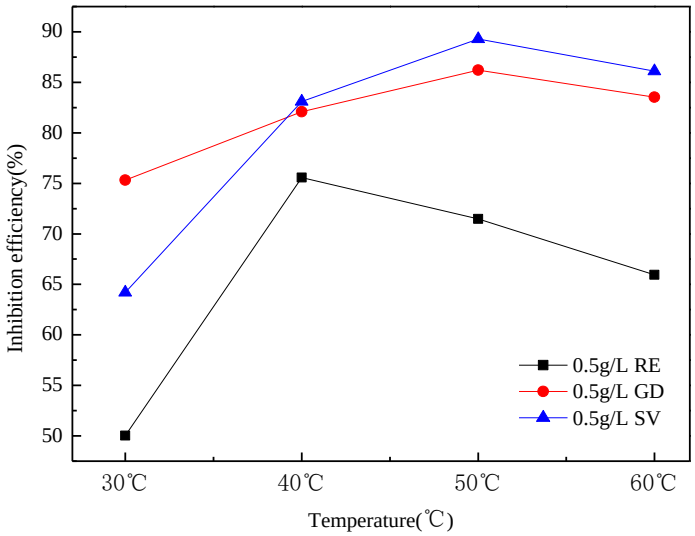

Figure 2. Relationship between temperature (from 30 ºC to 60 ºC) and inhibition efficiency for 0.5 g/L RE, GD, and SV by weight loss test.

Fig.3 shows that increasing concentrations of RE, GD, and SV at the same temperature leads to a gradual increase in inhibition efficiency. When the concentration of plant extract was 1 g/L at 30ºC, the inhibition efficiency was 91.76% for SV, 88.38% for GD, and 77.67% for RE. Increasing plant extract concentration leads to a greater effective inhibitor concentration, which leads to more adsorption on metal surface and a higher inhibition efficiency.

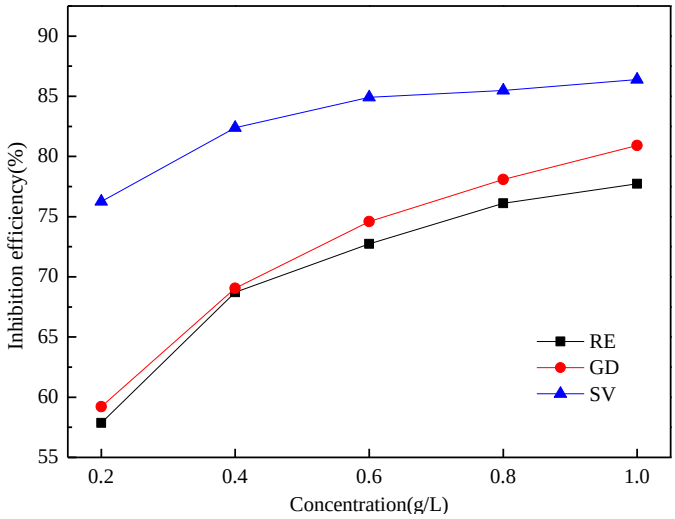

Figure 3. Relationship between inhibition efficiency and concentration for RE, GD, and SV at 30 ºC by weight loss test.

Fig.4 shows the graphs for the results of the electrochemical impedance spectroscopy (EIS) tests for RE, GD, and SV. They all show a similar semi-elliptical shape, which indicates that the only charge transfer occurs at the interface between the electrode and the corrosion solution during the corrosion of A3 steel electrode, and the process is not affected by the presence of corrosion inhibitors. The micro-inhomogeneity and roughness of the electrode surface lead to the dispersion of the interface impedance, which makes the semi-circular arc appear slightly flat [22]. With increasing RE, GD, and SV concentration, the radius of the semi-circular arc increases significantly, and the charge transfer resistance of the corrosion of A3 steel increases accordingly. This is because the extracts can be adsorbed on the surface of the electrode to form a film, which increases the resistance for charge transfer and makes it difficult for the anode metal to dissolve, so the corrosion resistance of the electrode is enhanced. Table 2 shows the results of data fitting for AC impedance.

η were defined with fitting data as:

$$\eta = \frac{R_{ct} - R_{ct0}}{R_{ct0}} \times 100\% \quad (4)$$

$$\eta = \frac{I_{corr} - I_{corr(inh)}}{I_{\text{corr}}} \times 100\% \quad (5)$$

R_{ct} (R_{ct0}) is the charge transfer resistance with (with not) corrosion inhibitors and $I_{corr(inh)}$ (I_{corr}) is the corrosion current density with (with not) corrosion inhibitors.

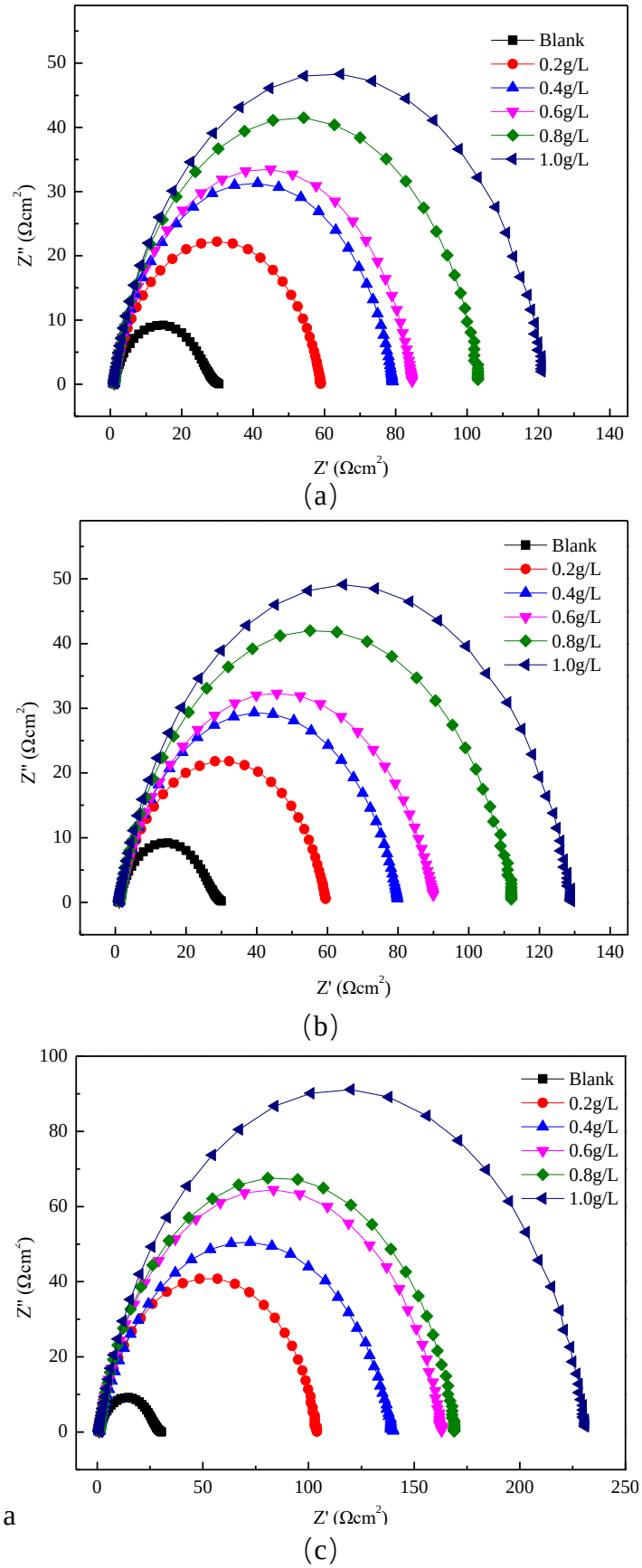

Figure 4. Graphs for the results of the electrochemical impedance spectroscopy (EIS) tests for RE(a), GD(b), and SV(c) with different concentration at 30 ºC.

Table 2. Under 30 ºC of A3 steel in different concentration of RE, SV, GD 1 mol/L HCl solution ac impedance parameters

	Concentration(g/L)	R_s(Ω▪cm^2)	R_{ct} (Ω▪cm^2)	C_{dl}(F▪cm^{-2})	η(%)
	Blank	1.17	24.46	1.44×10^{-3}	-
RE	0.2	0.93	58.05	1.91×10^{-4}	57.86
	0.4	1.01	78.16	1.75×10^{-4}	68.71
	0.6	1.10	83.56	1.60×10^{-4}	70.73
	0.8	0.97	102.40	1.04×10^{-4}	76.11
	1.0	1.07	120.70	1.11×10^{-4}	79.73
GD	0.2	1.10	58.54	3.33×10^{-4}	58.22
	0.4	1.02	79.02	2.38×10^{-4}	69.05
	0.6	1.08	89.28	2.57×10^{-3}	72.60
	0.8	1.05	111.60	1.60×10^{-3}	78.08
	1.0	1.09	128.10	1.29×10^{-4}	80.91
SV	0.2	0.85	103.00	1.04×10^{-4}	76.25
	0.4	0.91	138.80	1.57×10^{-4}	82.38
	0.6	0.81	162.10	1.30×10^{-4}	84.91
	0.8	0.96	168.40	7.26×10^{-5}	85.48
	1.0	0.91	230.50	1.36×10^{-4}	89.39

Table 2 data shows that the charge transfer resistance (R_{ct}) of the three plant inhibitors increased significantly with increasing RE, GD, and SV concentration, and the inhibition efficiency (η) increased gradually with increasing RE, GD, and SV concentration. The inhibition efficiency of the three plant inhibitors prepared in this experiment was RE < GD < SV at the same concentration.

Fig. 5 shows that the anode and cathode parts of the polarization curves for RE, GD, and SV are shifted downward to different degrees, indicating that the reaction of the two poles during corrosion process is effectively suppressed. The inhibition effect increases with increasing concentration of RE, GD, and SV. The inhibition effect of the cathodic reaction is more obvious than that of the anode reaction, so RE, GD, and SV are cathodic inhibitors for plant corrosion.

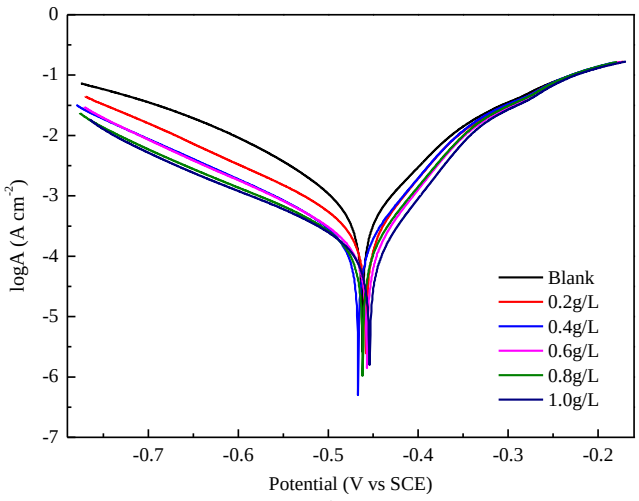

（a）

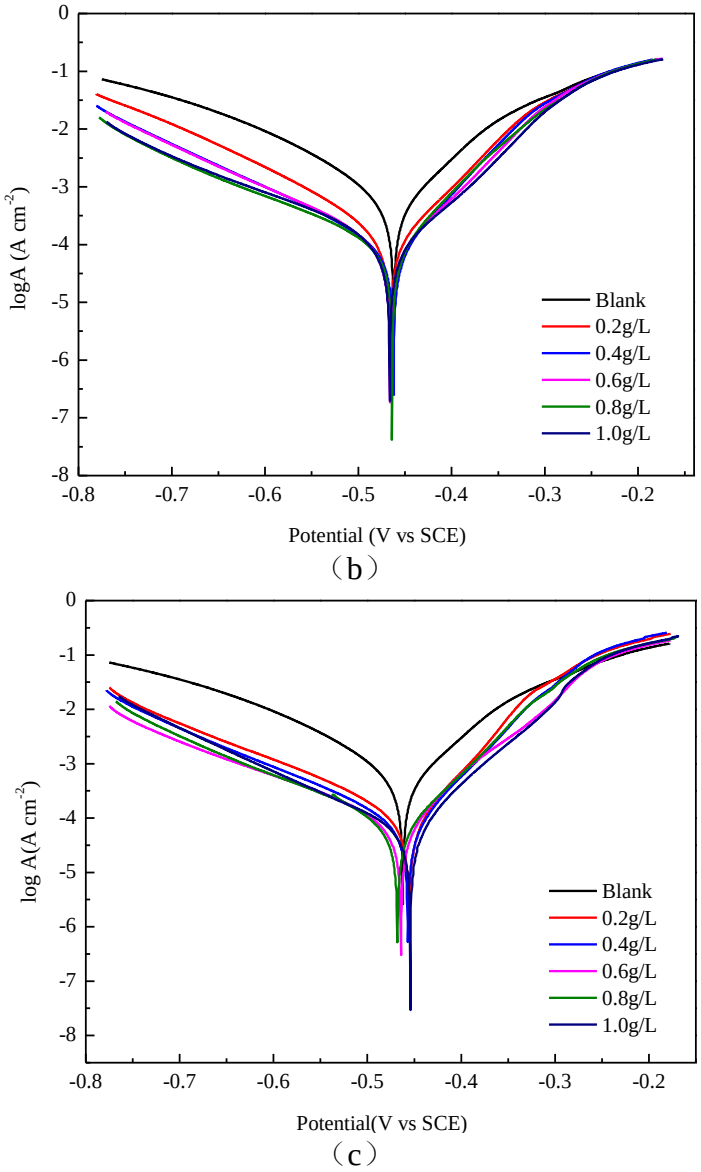

Figure 5. Polarization curves for RE(a), GD(b), and SV(c) with different concentration at 30 ºC.

Table 3 shows that the corrosion current density (I_{corr}) decreased gradually with increasing RE, GD, and SV concentrations, and the corrosion inhibition efficiency gradually increased. At the highest concentration of RE, GD, and SV, which was 1 g/L in our tests, the corrosion current density reached 77.67%, 88.38%, and 91.76%, respectively. The E_{corr} < 85 mV indicated that SV, GD, and RE are all mixed inhibitors [23]. It can be inferred that the adsorption mechanism of their inhibition was the geometric coverage effect [24]. The anodic dissolution reaction and cathodic hydrogen evolution reaction of A3 steel in a corrosive medium can be effectively inhibited by SV, GD and RE. The corrosion potential remained basically unchanged, indicating that the geometric blocking effect was stronger than the energy effect in the adsorption process, so the main mechanism of corrosion inhibition was the geometric blocking mechanism [25]. The effective corrosion inhibitor adsorbed on the surface acts as a

barrier, reducing the metal surface area involved in the reaction, and the corrosion inhibitor adsorbed evenly, indicating that the adsorption mode was a non-localized adsorption.

Table 3. Under 30 ℃, A3 steel in different RE、GD、SV concentration 1 mol/L HCl solution of polarization curve parameters

	Concentration g/L	$-E_{corr}$ mV	I_{corr} μA·cm^{-2}	b_a mV/decade	$-b_c$ mV/decade	η %
	blank	462	843.65	108	141	-
	0.2	458	420.12	93	157	50.2
	0.4	466	283.21	88	161	66.4
RE	0.6	457	235.37	84	161	72.1
	0.8	461	235.94	85	178	72.0
	1.0	454	188.36	81	179	77.7
	0.2	466	166.14	82	123	80.3
	0.4	462	108.53	75	142	87.1
GD	0.6	466	102.13	77	136	87.9
	0.8	464	115.65	77	171	86.3
	1.0	466	98.73	78	150	88.4
	0.2	455	129.12	73	152	84.7
	0.4	457	94.27	69	147	88.8
SV	0.6	464	87.62	75	162	89.6
	0.8	468	81.58	72	148	90.3
	1.0	454	69.56	69	141	91.8

A comparison of the SEM images in Fig.6(a), 6(d), and 6(g) show that the corrosion pits on the surface of A3 steel decreased significantly after adding SV, and the roughness of the steel surface decreased with an increase in SV concentration [26,27]. Therefore, the corrosion of A3 steel in a 1 mol/L HCl solution was effectively inhibited by the formation of a protective SV film on the surface of the A3 steel. The larger the adsorption area of the SV corrosion inhibiting molecules, the smaller the contact area between steel and the hydrochloric acid solution, which can effectively blocks the corrosion reaction and greatly improve the corrosion inhibiting efficiency [28]. RE and GD can be analyzed in the same way. The surface smoothness of A3 steel with the same concentration was SV > GD > RE.

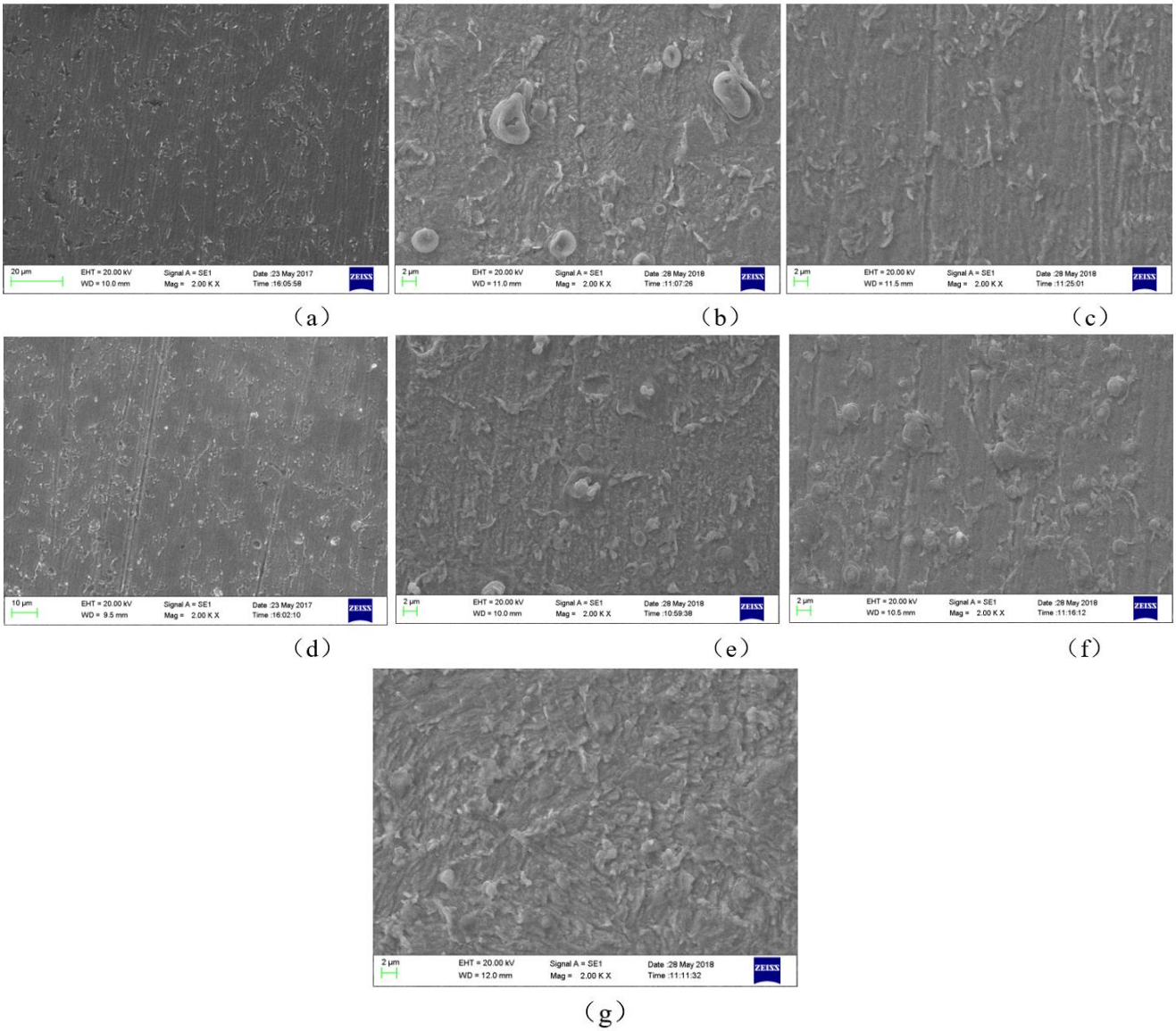

Figure 6. SEM images for adding different concentration of SV, RE, and GD at 30 ºC by weight loss test. ((a) 0.2 g/L SV, (b) 0.2 g/L RE, (c) 0.2 g/L GD, (d) 1.0 g/L SV, (e) 1.0 g/L RE, (f) 1.0 g/L GD, (g) blank)

We next explored the inhibition efficiencies of mixtures of inhibitors. Fig.3 showed that the corrosion inhibition efficiency of RE at the same concentration was lower than that of GD and SV and that increasing RE, GD, and SV concentrations led to increased corrosion inhibition efficiency of A3 steel. When the concentration of RE was 0.8 g/L, an inflection point appeared. Beyond this point, increasing RE concentration had no obvious effect on the corrosion inhibition efficiency. Therefore, 0.8 g/L was chosen as the optimal compound concentration of RE. Mixtures of RE and GD (RG) with the mass ratios RE:GD = 1:1, 1:2, 1:3, 1:4 and mixtures of RE and SV (RS), with the mass ratios RE:SV = 1:1, 1:2, 1:3, 1:4 were prepared. The compounding synergies S_I were defined as:

$$S_I = \frac{1-\eta_A-\eta_B+\eta_A\eta_B}{1-\eta_{A+B}} \qquad (6)$$

η_A (η_B, η_{A+B}) was the corrosion inhibition efficiency of A (B, A+B) solution.

Fig. 7 shows the corrosion inhibition effects of the mixture RG were better than that of RE and GD alone at the same concentration. When the RE:GD = 1:4, the corrosion inhibition efficiency of RG reached 87.71%.

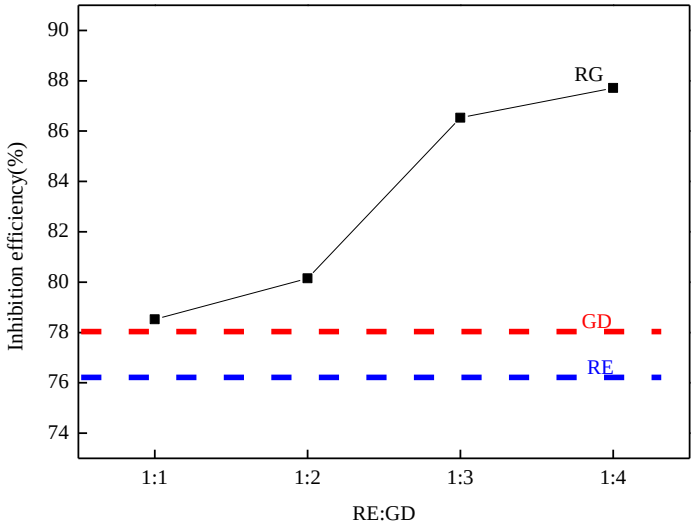

Figure 7. Inhibition efficiencies of 0.8 g/L RE, GD, and the mixture RG with different ratios at 30 ºC by weight loss test.

Fig. 8 shows that the corrosion inhibition effects of the mixture RS were better than that of the same concentration of RE and SV alone. When RE:SV=1:1, the maximum inhibition efficiency was 91.92%.

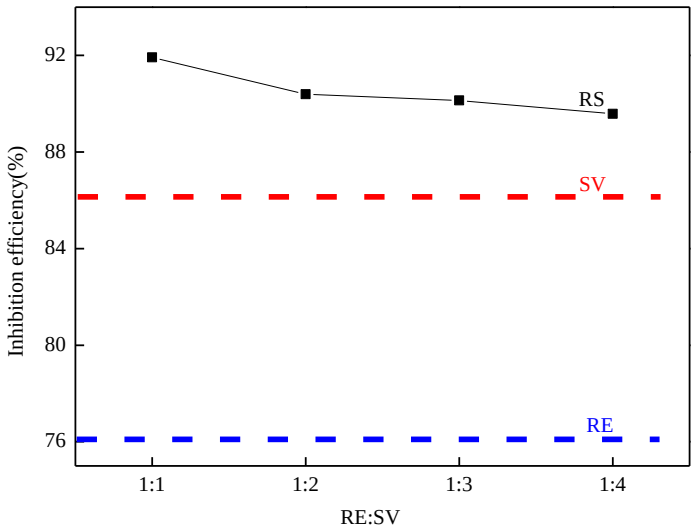

Figure 8. Inhibition efficiencies of 0.8 g/L RE, SV, and the mixture RS with different ratios at 30 ºC by weight loss test.

Table 4. In 30 ℃, 1 mol/L HCl solution RE after the corrosion of synergies with GD factor (S_I)

RE:GD	η_{RE} %	η_{GD} %	η_{RG} %	S_I
1:1	76.1	78.1	78.5	0.24
1:2			80.2	0.26
1:3			86.5	0.39
1:4			87.7	0.43

Table 5. In 30 ℃, 1 mol/L HCl solution RE after the corrosion of synergies with SV factor (S_I)

RE:SV	η_{RE}/%	η_{SV}/%	η_{RS}/%	S_I
1:1	76.1	85.5	91.9	0.43
1:2			90.4	0.36
1:3			90.1	0.35
1:4			89.6	0.33

Eq.(6) was used to calculate S_I, and the results are shown in Table 5., shown in tables 4 and 5. the S_I values for the mixture of RE and GD in 1 mol/L HCl solution were less than 1, and the S_I values for the mixture of RE and SV in 1 mol/L HCl solution were also less than 1. This shows that these mixtures have a good synergistic effect on corrosion inhibition. Their synergistic action of competitive adsorption leads to a significant increase in the inhibition efficiency.

4. CONCLUSION

In this paper, Solanum violaceum fruit, gardenia petals and rose petals were extracted by the Soxhlet extraction method and used as corrosion inhibitors for the corrosion of A3 steel in 1 mol/L HCl solution. The main conclusions are:

(1) The polar groups with N, O, and S of SV, GD, and RE are thought to be the primary inhibition groups.

(2) When the temperature was 30 ºC and the concentration of each inhibitor was 1 g/L, the inhibition efficiency was the highest with 91.76% for SV, 88.38% for GD, and 79.73% for RE, showing that SV, GD, and RE are all natural plant corrosion inhibitors.

(3) When the mass ratio of RE:GD was 1:4, the corrosion inhibition efficiency of 0.8 g/L RG was 87.71%. When the mass ratio of RE:SV was 1:1, the corrosion inhibition efficiency of 0.8 g/L RS was 91.92%, which was higher than that of 0.8 g/L RE, GD, and SV alone. The corrosion inhibition ability of single plant inhibitor RE was greatly improved by the mixture with GD or SV.

ACKNOWLEDGEMENTS
This work was supported by the National Natural Science Foundation of China (No. 51774242).

References

1. X. Zhao, J. Yang and X.Q. Fan, *Appl. Mech. Mater*., 44-47(2011)4063.
2. J. Zheng, Y.N. Wang, B.L. Zhang, T. Yang, X.M. Jiao and Y. He, *Corros. Sci. Prot. Technol*., 23(2011)103.
3. P.B. Raja, M.G. Sethuraman, Mater. Lett., 62(2008)113.
4. P.P. Kong, N.L. Chen, D.Z. Bai, Y.Y. Wang, Y. Lu, and H.X. Feng, *J. Chin. Soc. Corros. Prot*., 38(2018) 409.
5. K. Haruna, I.B. Obot, N.K. Ankah, A.A. Sorour and T.A. Saleh*, J. Mol. Liq*., 264(2018)515.
6. S.A. Umoren, A.A. Alahmary, Z.M. Gasem and M.M. Solomon, *Int. J. Biol. Macromol*., 117(2018)1017.
7. P. Muthukrishnan, P. Prakash, B. Jeyaprabha and K. Shankar, *Arabian J. Chem*., 28(2015)1.
8. H. Mohammed, S.B. Sobri, *Mater. Lett*., 229(2018)82.
9. A.S. Yaro, A.A. Khadom and H.F. Ibraheem, *Anti-Corros. Methods Mater*., 58 (2011)116.
10. X. Wang, S.F. Ren, H. Jiang, L. Hou and W.J. Zhou, *Surf. Technol*., 47(2018)196.
11. F.B. Mainier and R.D.M.B.E. Silva, *Anti-Corros. Methods Mater*., 62(2015)241.
12. C.N. Li, Surf. Technol., 45(2016)80.
13. C. Verma, E.E. Ebenso, I. Bahadur and M.A. Quraishi, *J. Mol. Liq.,* 266(2018)577.
14. S.S.D.A.A. Pereira, M.M. Pegas, T.L. Fernandez, and M. Magalhaes, T.G. Schontag, D.C. Lago, L.F.D.Senna and E.D. Elia, *Corros. Sci*., 65(2012)360.
15. M. Jokar, T.S. Farahani and B. Ramezanzadeh, *J. Taiwan Inst. Chem. Eng*., 63(2016)436.
16. F.P. Yi, J. Sun, X.L. Bao, B.D. Ma and M. Sun, *LWT--Food Sci. Technol*., 102(2019)310.
17. Z.B. Xiao, J. Li, Y.W. Niu, Q. Liu and J.H. Liu, *Nat. Prod. Res*., 31(2017)2294.
18. X.B. Li, M. Ma, X.G. Zhang, L. Deng, Y.R. Wang, Z. Bian, S.N. Cai, B.Y. Peng, J.Q. Yang and Y. Chen, *Exp. Ther. Med.,* 14(2017)1381.
19. Z.B. Liu, J.G. Chen, Z.P. Yin, X.C. Shangguan, D.Y. Peng, T. Lu and P.Lin, Plant Cell, *Tissue Organ Cult.,* 134(2018)79.
20. J.Y. Fang, B. Yang, Z.W. Ge, X. Bai and B.J. Yan, *J. Sep. Sci*., 40(2017)3923.
21. A.S. Koushik, K.M.I. Huque, B.M. Mustahsan and H.M. Salim, *Marmara Pharm. J*., 22(2018)96.
22. C.I. Min, H. Venkatesan, P. Kanchana, A. Natrajan, C. Subramanian, H.Y. Chi, K.S. Hyun and P. Mayakrishnan, *J. Electrochem. Sci. Technol*., 9(2018)238.
23. J.M. Ju, A.N. Ren and H.Y. Yuan. Lishizhen *Med. Mater. Med. Res*., 9(1998)332.
24. M.D. Li, C.L. Dai, B. Yang, Y. Qiao and Z.P. Zhu, *J. Mater. Eng. Perform*., 26(2017)764.
25. K.V. Kumar and B.V.A. Rao, New *J. Chem*., 41(2017)6278.
26. M. Xia, P.L. Guan, K. Gong, X.Y. Sun, F. Ren and D.F. Shen, *Corros. Sci. Prot. Technol*., 25(2013)495.
27. X.H. Li, H. Fu and S.D. Deng, *J. Chin. Soc. Corros. Prot*., 31(2011)149.
28. X. Wang, S.F. Ren, D.X. Zhang, H. Jiang and Y. Gue, *Int. J. Electrochem. Sci*., 13(2018)9888.